

## **NOTE**

This online version of the thesis may have different page formatting and pagination from the paper copy held in the University of Wollongong Library.

## **UNIVERSITY OF WOLLONGONG**

### **COPYRIGHT WARNING**

You may print or download ONE copy of this document for the purpose of your own research or study. The University does not authorise you to copy, communicate or otherwise make available electronically to any other person any copyright material contained on this site. You are reminded of the following:

Copyright owners are entitled to take legal action against persons who infringe their copyright. A reproduction of material that is protected by copyright may be a copyright infringement. A court may impose penalties and award damages in relation to offences and infringements relating to copyright material. Higher penalties may apply, and higher damages may be awarded, for offences and infringements involving the conversion of material into digital or electronic form.

## Chapter 5

### Isolation of Novel Compounds from Human Cataract Lenses

#### 5.1 Introduction

The aim of this work was to determine if acid hydrolysis of cataract proteins could be a useful technique for isolating novel compounds. If so, their identification would provide information about the changes that result in ARN cataract. In addition, the aim was to determine if there was any evidence for the presence of 3OHKyn or Kyn fragment ions in these novel peaks, that elute in the HPLC of acid digests. The data presented in Chapter 3 of this thesis together with previous data show that all three Kyn UV filters, 3OHKynG, 3OHKyn and Kyn, are attached to normal older lens proteins.<sup>101,103</sup> Table 5.1 lists the characteristic ions of 3OHKyn and Kyn amino acid adducts. In addition, the UV-visible wavelength maxima are also listed for each adduct. The ions highlighted in bold were used as ‘signature’ ions in this study.

**Table 5.1** List of characteristic ions, and absorbance maxima for each of the 3OHKyn and Kyn amino acid adducts.<sup>103</sup>

Previously in Chapter 3, CLP and normal human aged lens protein were hydrolysed with acid in the presence of antioxidants. Figure 5.1A and Figure 5.1B are the HPLC profiles of the hydrolysed CLP and hydrolysed normal aged human lens protein respectively (these HPLC profiles have previously been shown in Figure 3.5A and 3.6B respectively of this thesis). As a comparison, a number of human ARN cataract lens proteins were hydrolysed under the same conditions, and Figure 5.1C shows a

representative HPLC profile of the hydrolysate of human cataractous lens protein. Human cataractous nuclei that appeared very Dark (*i.e.* Types III or IV, Pirie classification<sup>161</sup>) were used for this study. The absorbance was monitored at 360 nm to simplify the profiles, and to assist in identifying UV filter modification sites. The HPLC profile of human cataractous lens protein (Figure 5.1C) was found to exhibit numerous peaks that were not present in calf or normal human lens hydrolysates (Figure 5.1A and Figure 5.1B).

The peaks that were collected and examined were, P1, which eluted at 27.0 min, P2 eluted at 31.1 min, P3 eluted at 32.2 min, and P4, P5 and P6 eluted at 36.0 min, 37.5 min and 45.0 min respectively (Figure 5.1C). Numerous lenses (60) were hydrolysed and individual peaks were pooled in order to obtain sufficient quantities for analysis of each peak by mass spectrometry, UV-visible spectroscopy and NMR spectroscopy. It was found that each peak required a number of purifications by HPLC to ensure purity.

Numerous studies were undertaken to find the best approach for purifying these peaks further. Attempts were made to purify these peaks by HPLC. Various gradients were used and several columns including C8 and C18 columns of various lengths were used. The method that was finally settled upon and gave best separation involved taking the peaks from the first stage of HPLC, where the buffers contained TFA, drying these fractions, and performing HPLC using a different column (Synergi Fusion). A different gradient was used to separate each of P1-P6, and formic acid was used instead of TFA in the buffers. The analysis of P1, P2, P3, P4, P5 and P6 is summarised in Section 5.3.

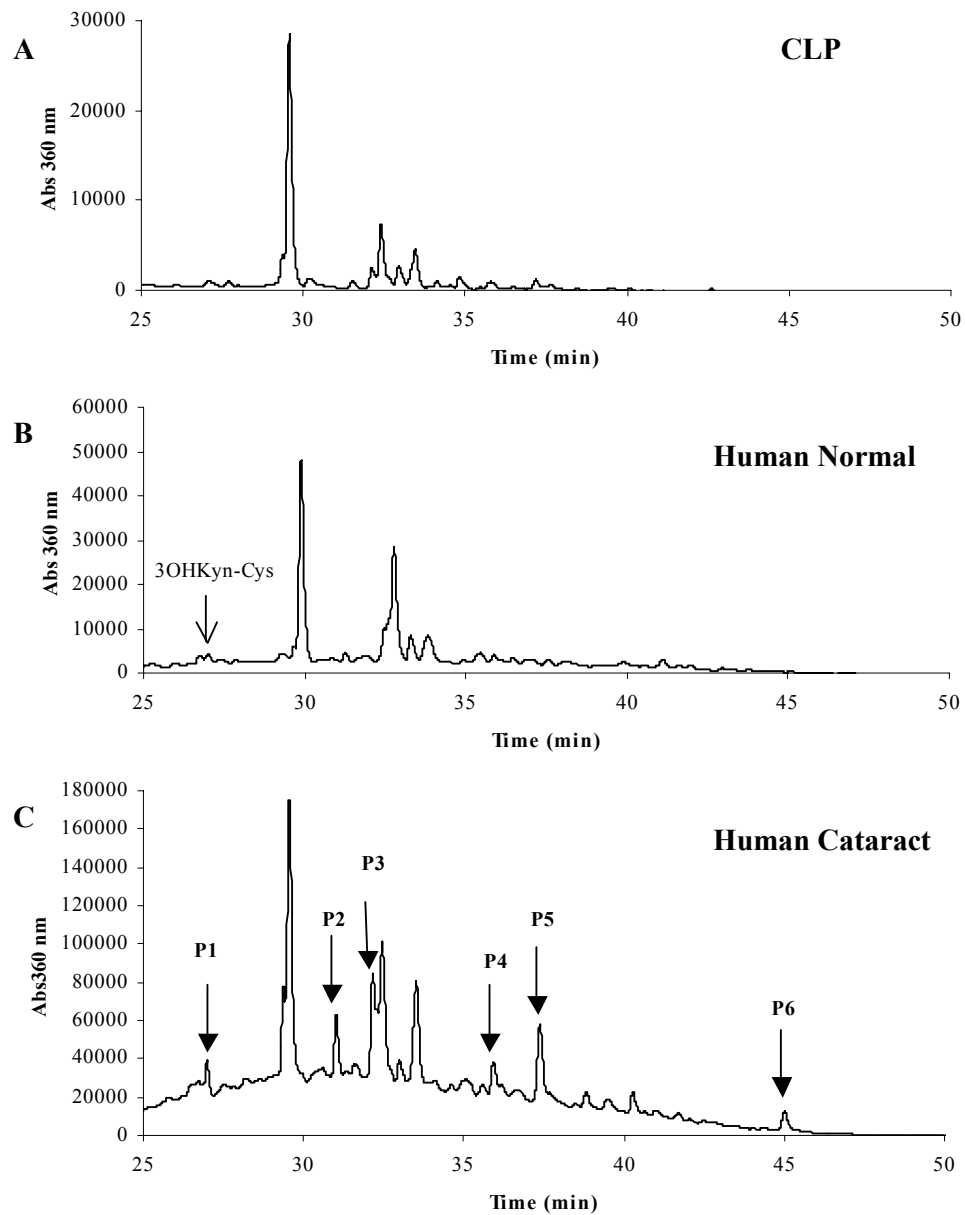


**Figure 5.1** HPLC chromatograms of acid hydrolysed lens protein samples (~ 1 mg hydrolysed protein was injected in each case). *A*, CLP; *B*, Normal human lens nuclear protein, from a 76 year old lens; *C*, Pooled human cataract lens nuclear protein. The HPLC profiles of all human cataract lens protein hydrolysed were consistent.

## 5.2 Materials and Methods

### 5.2.1 Materials

All organic solvents and acids were HPLC grade (Ajax, Auburn, NSW, Australia). Milli-Q<sup>®</sup> water (purified to 18.2 M $\Omega$ /cm<sup>2</sup>) was used in the preparation of all solutions. Formic acid, heptafluorobutyric acid, HCl (6 M, sequencing grade), TFA, thioglycolic acid and phenol were obtained from Sigma-Aldrich Chemical Co. (St. Louis, MO, U.S.A.)

### 5.2.2 Preparation of Cataract Lens Protein

ARN cataract lenses were obtained from K.T. Sheth Eye Hospital, Rajkot, Gujarat, India. Nuclei were obtained using a cork borer (5 mm), and the ends were removed (1 mm). The nuclei were extracted with 80% (v/v) ethanol once, and the insoluble protein was freeze dried and stored at 4<sup>0</sup>C.

### 5.2.3 Hydrolysis of Cataract Lens Protein

Each extracted nucleus was hydrolysed with 6 M HCl (1 mL), thioglycolic acid (5% v/v) and phenol (1% w/v) in an evacuated hydrolysis tube for 24 hours at 110<sup>0</sup>C. The samples were freeze dried and dissolved in 0.1% (v/v) aqueous TFA and analysed by HPLC. 60 cataract nuclei were hydrolysed for purification.

### 5.2.4 First Stage of HPLC Purification

RP-HPLC was performed on a Shimadzu HPLC system. For analytical scale separations, a Phenomenex column (Jupiter C18, 300 Å, 5  $\mu$ m, 4.6 x 250 mm) was used with the following mobile phase conditions: solvent A (aqueous 0.1% (v/v) TFA) for 5 minutes followed by linear gradient of 0-50% solvent B (80% (v/v) acetonitrile/H<sub>2</sub>O, 0.1% (v/v) TFA) over 20 minutes followed by a linear gradient of 50-100% B over 15 minutes and re-equilibration in the aqueous phase for 15 minutes. The flow rate was 0.5 mL/min. Six peaks (P1, P2, P3, P4, P5 and P6) were collected. Absorbance was monitored at 360 nm.

### 5.2.5 Second Stage of HPLC Purification

The 6 peaks collected were rerun on the Shimadzu HPLC system. Several test chromatograms were used to determine the best conditions for purification of each of the peaks P1-P6. Analytical separations were with a Phenomenex Synergi Fusion reversed phase column (C18, 80 Å, 4 µm, 3.0 x 150 mm). The flow rate was 0.4 mL/min, and the HPLC solvents were as follows: solvent A (aqueous 0.1% (v/v) formic acid) and solvent B (80% (v/v) acetonitrile/H<sub>2</sub>O, 0.1% (v/v) formic acid). The individual gradients for each of P1, P2, P3, P4, P5 and P6 are listed below. Absorbance was monitored at 360 nm.

#### 5.2.5.1 HPLC Gradient for P1

The following mobile phase conditions were used to purify P1: solvent A for 8 minutes followed by linear gradient of 0-15% B over 12 minutes followed by a linear gradient of 15-60% B over 20 minutes, 60-100% B over 5 minutes and re-equilibration in the aqueous phase for 15 minutes.

#### 5.2.5.2 HPLC Gradient for P2, P3, P4 and P5

The following mobile phase conditions were used to purify P2, P3, P4 and P5: solvent A for 8 minutes followed by linear gradient of 0-45% B over 7 minutes followed by a linear gradient of 45-100% B over 30 minutes, and re-equilibration in the aqueous phase for 15 minutes.

#### 5.2.5.3 HPLC Gradient for P6 (second HPLC purification)

A Phenomenex Luna column (C8, 100 Å, 3 µm, 2.0 x 150 mm) was used. The following mobile phase conditions were used to purify P6: solvent A (aqueous 0.2% (v/v) heptafluorobutyric acid) for 8 minutes followed by linear gradient of 0-30% solvent B (80% (v/v) acetonitrile/H<sub>2</sub>O, 0.2% (v/v) heptafluorobutyric acid) over 7 minutes followed by a linear gradient of 30-70% B over 20 minutes, and a linear gradient of 70-100% B over 10 minutes, and re-equilibration in the aqueous phase for 15 minutes. The flow rate was 0.2 mL/min.

#### **5.2.5.4 HPLC Gradient for P6 (third HPLC purification)**

A Phenomenex Synergi Fusion column (C18, 80 Å, 4 µm, 3.0 x 150 mm) was used. The following mobile phase conditions were used: solvent A (aqueous 0.1% (v/v) formic acid) at 95% for 5 minutes followed by linear gradient of 5-20% solvent B (80% (v/v) acetonitrile/H<sub>2</sub>O, 0.1% (v/v) formic acid) over 10 minutes followed by a linear gradient of 20-80% over 20 minutes, and a linear gradient of 80-100% B over 5 minutes, and re-equilibration in the aqueous phase for 15 minutes. The flow rate was 0.2 mL/min

#### **5.2.6 Mass Spectrometry**

See Section 2.2.10 for details.

#### **5.2.7 Tandem Mass Spectrometry (MS/MS)**

See Section 2.2.11 for details.

#### **5.2.8 High Resolution Mass Spectrometry**

See Section 2.2.12 for details.

#### **5.2.9 NMR Spectroscopy**

See Section 2.2.13 for details.

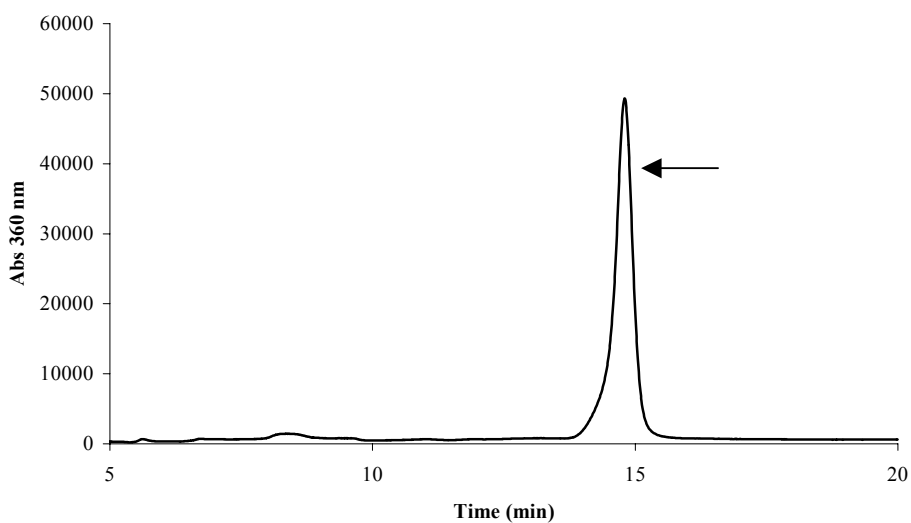
#### **5.2.10 UV-visible Spectroscopy**

See Section 2.2.14 for details.

### 5.3 Results

#### 5.3.1 Analysis of P1

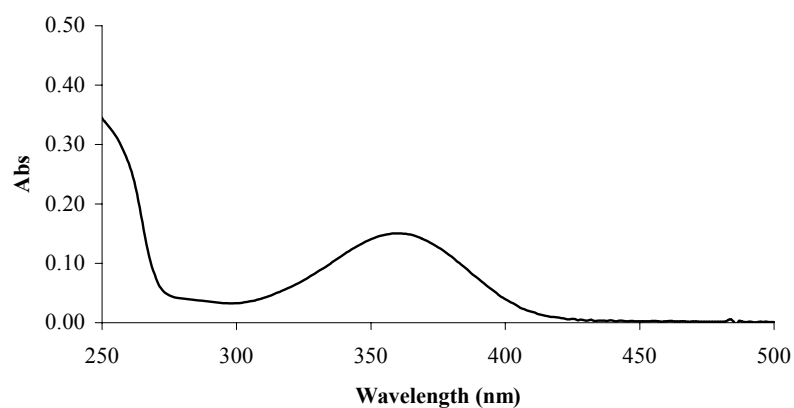
Acid hydrolysis of human cataract lenses yielded P1 eluting at 27.0 min (Figure 5.1C). Since it did not elute as a very sharp peak, further purification was necessary. After several trials, P1 was further purified by HPLC using buffers containing 0.1% (v/v) formic acid and a Phenomenex Synergi Fusion column. Figure 5.2 shows the partial HPLC profile of the second phase of HPLC purification. Repurified P1 eluted as a single peak at 14.7 min (Figure 5.2). This peak was collected for UV-visible and mass spectral analysis.



**Figure 5.2** HPLC chromatogram of P1 after a second purification stage using a Phenomenex Synergi Fusion column, and 0.1% (v/v) formic acid HPLC buffers.

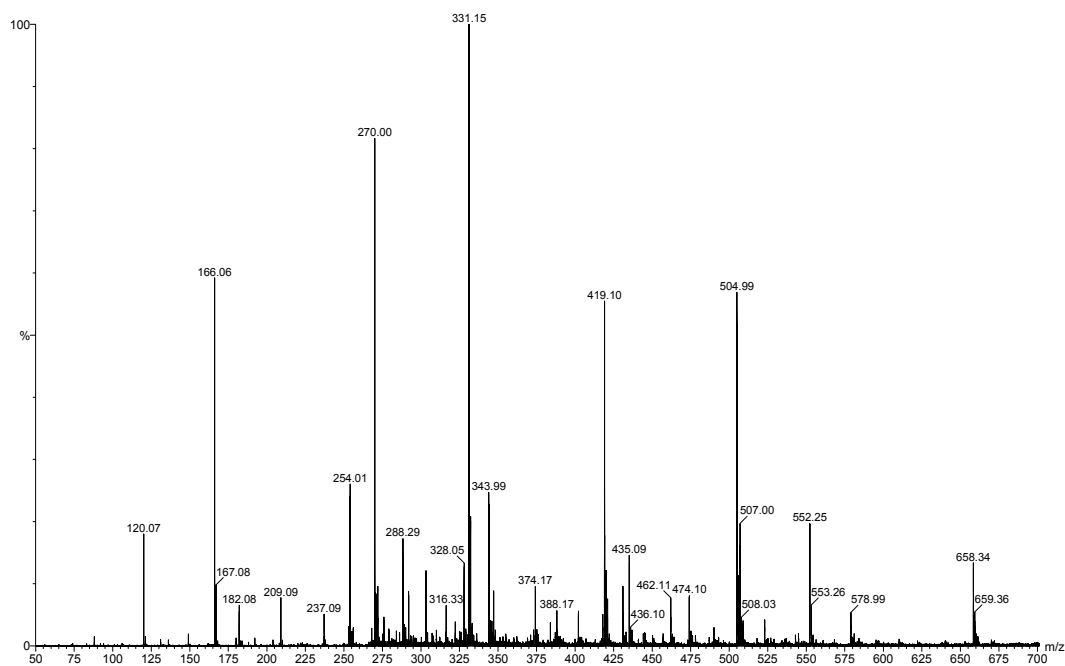


A UV-visible spectrum of the peak eluting at 14.7 min in Figure 5.2 shows that this product displays a broad peak with maximum absorbance centred at 360 nm (Figure 5.3). 3OHKyn amino acid adducts and Kyn amino acid adducts all have broad peaks with maximum UV absorbances centred at 365 nm.<sup>103</sup> The UV spectrum (Figure 5.3) indicates that the product could be a UV filter derivative.



**Figure 5.3** UV-visible spectrum of the peak eluting at 14.7 min in Figure 5.2.

The ESI mass spectrum of the peak eluting at 14.7 min in Figure 5.2 is shown in Figure 5.4. There were no ions greater than  $m/z$  700. The largest ion observed was  $m/z$  658, and the most abundant ion at  $m/z$  331. The mass spectrum (Figure 5.4) did not exhibit any of the signature ions listed in Table 5.1, *i.e.* Figure 5.4 does not have ions that correspond to the ions of 3OHKyn and Kyn amino acid adducts. MS/MS was conducted on some of the ions.

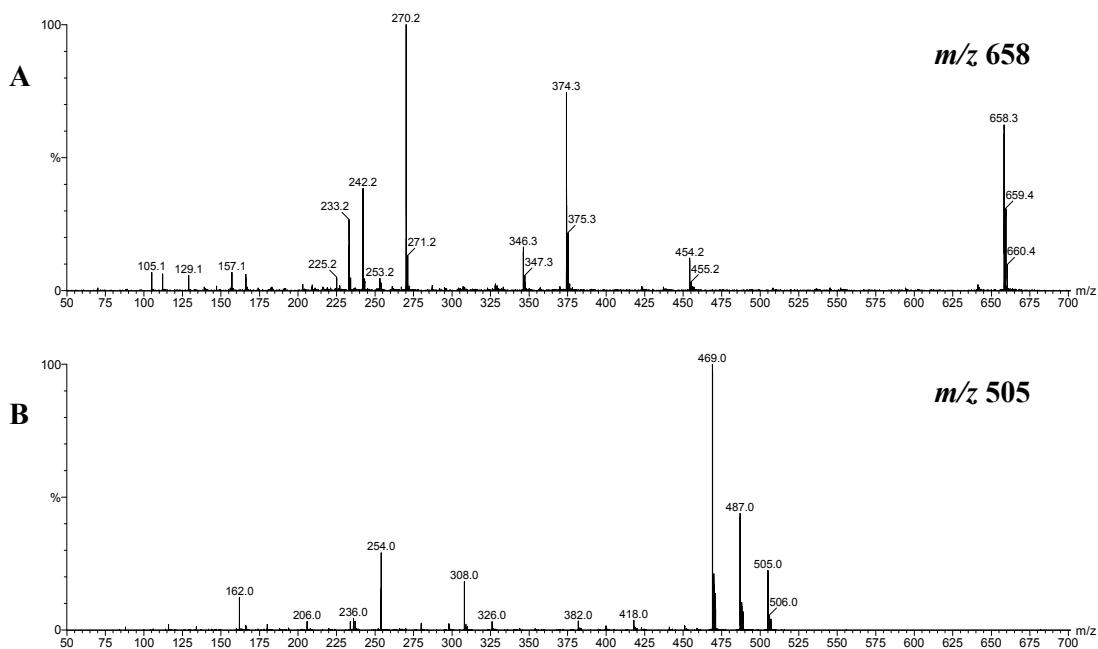


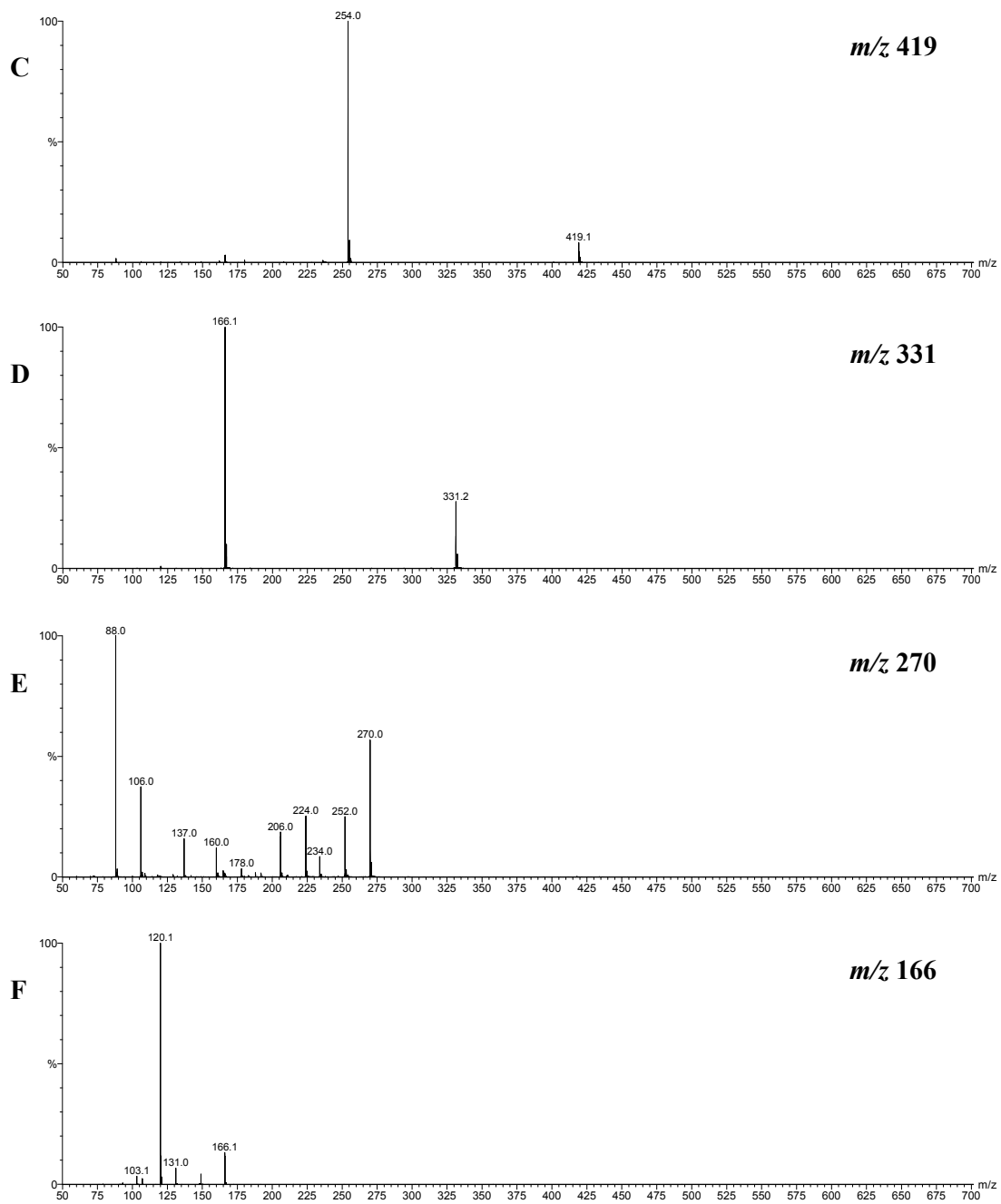
**Figure 5.4** ESI mass spectrum of the peak eluting at 14.7 min in Figure 5.2.

Figure 5.5A shows the MS/MS spectrum of ion  $m/z$  658. The major fragment ions include  $m/z$  641 (loss of  $m/z$  17), 454, 374, 346, 270, 242, and 233. None of these ions correspond to UV filter fragment ions. Figure 5.5B shows the MS/MS spectrum of ion  $m/z$  505. The major fragment ions include  $m/z$  487 (loss of  $m/z$  18), 469 (loss of  $m/z$  18), 418, 382, 326, 308, 254, 236, 206 and 162. Again none of these ions were UV filter fragment ions. A loss of  $m/z$  18 normally is due to the loss of water.<sup>225</sup>

Figure 5.5C shows the MS/MS spectrum of ion  $m/z$  419. The major fragment ions include  $m/z$  254 and 166. Figure 5.5D shows the MS/MS spectrum of ion  $m/z$  331. The fragment ions include  $m/z$  166 and 120. Figure 5.5E shows the MS/MS spectrum of ion  $m/z$  270. Fragment ions include  $m/z$  252, 234, 224, 206, 178, 160, 137, 106 and 88. Finally, Figure 5.5F shows the MS/MS spectrum of ion  $m/z$  166. The fragment ions included  $m/z$  149, 131, 120, 107 and 103.

A summary of the major ions for each of P1-P6, together with the MS/MS data, is shown in Table 5.2.

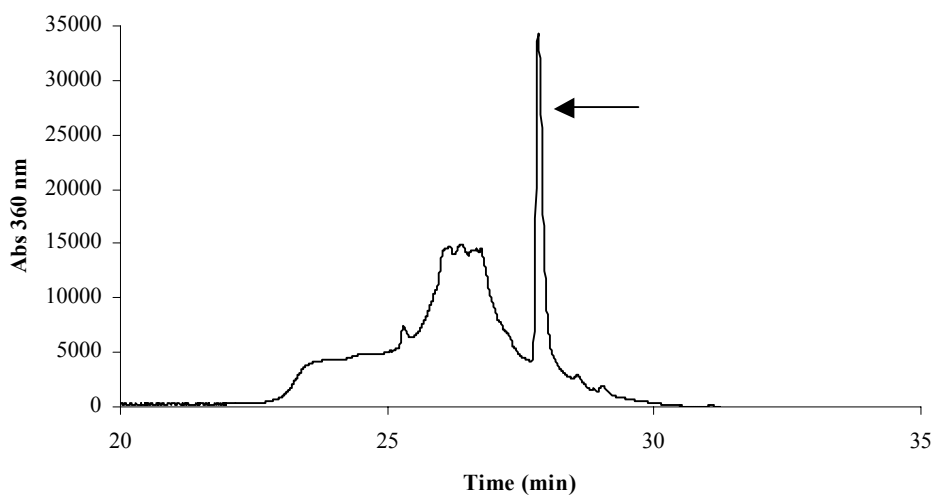




**Figure 5.5** MS/MS spectra. MS/MS of ions that were present in the ESI mass spectrum (Figure 5.4). *A*,  $m/z$  658; *B*,  $m/z$  505; *C*,  $m/z$  419; *D*,  $m/z$  331; *E*,  $m/z$  270; *F*,  $m/z$  166.

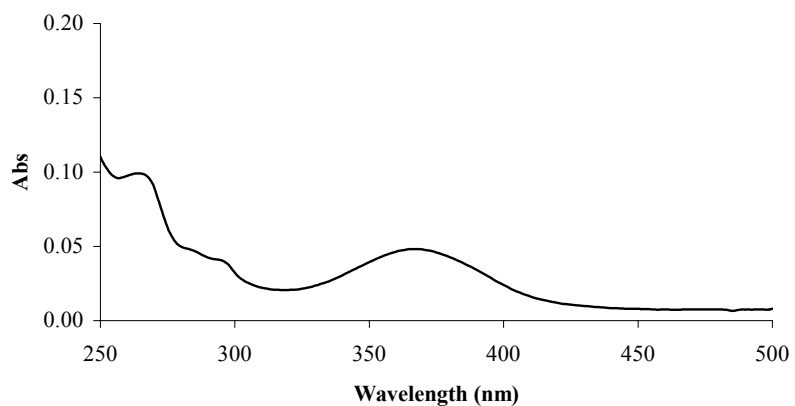
### 5.3.2 Analysis of P2

Acid hydrolysis of human cataract lenses also yielded P2 eluting at 31.1 min (Figure 5.1C). This peak eluted as a medium-sized peak. P2 was further purified under the same conditions as P1 *i.e.* Phenomenex Synergi Fusion, and formic acid HPLC buffers. A different gradient on the HPLC system was used (see Section 5.2.5.2). Figure 5.6 shows the partial HPLC profile of the second phase of HPLC purification. In the second stage of HPLC, P2 eluted as a broad peak followed by a sharp peak eluting at 27.8 min (Figure 5.6). The sharp peak was collected for UV-visible and mass spectral analysis.



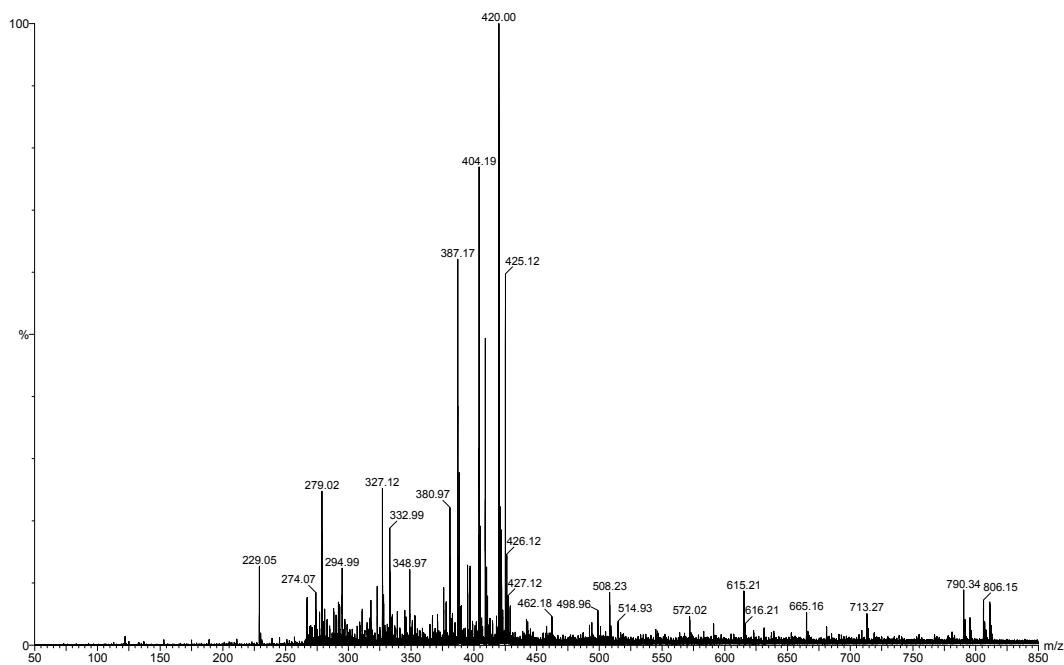
**Figure 5.6** HPLC chromatogram of P2 after a second purification stage using a Phenomenex Synergi Fusion column, and 0.1% (v/v) formic acid HPLC buffers.

A UV-visible spectrum of the peak eluting at 27.8 min in Figure 5.6 shows that this product has a broad peak with a maximum absorbance centred at 368 nm (Figure 5.7). The UV-visible spectrum (Figure 5.7) indicates that the product could be a UV filter derivative, since 3OHKyn and Kyn amino acid adducts have broad peaks with UV absorbances centred at 365 nm.<sup>103</sup>



**Figure 5.7** UV-visible spectrum of the peak eluting at 27.8 min in Figure 5.6.

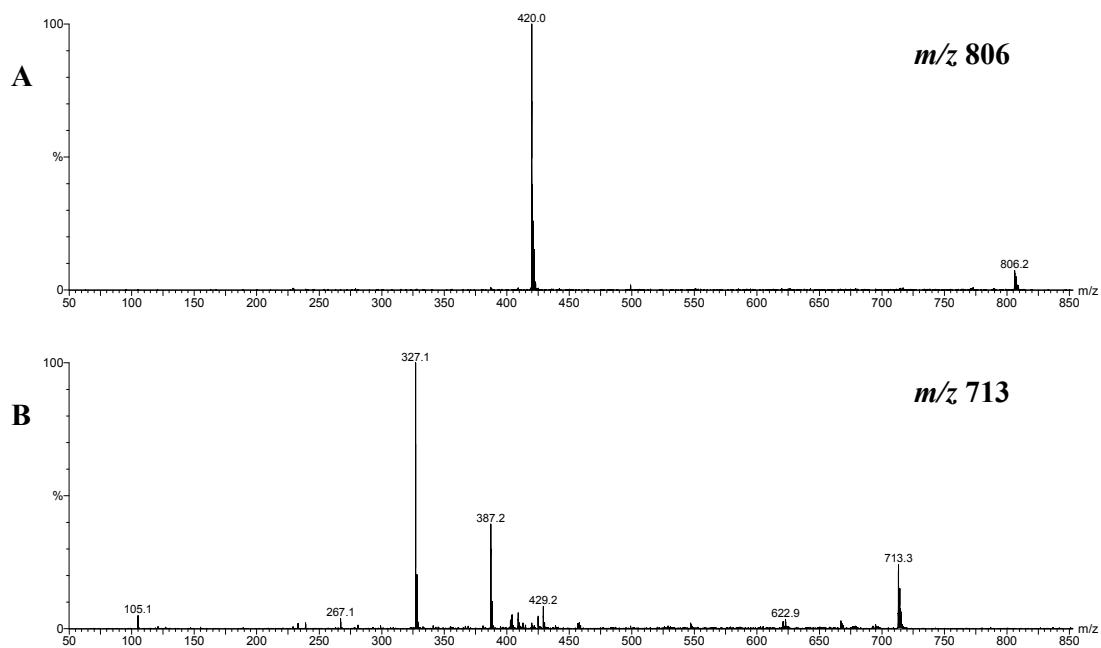
The ESI mass spectrum of the peak eluting at 27.8 min (Figure 5.6) is shown in Figure 5.8. There were no ions greater than  $m/z$  850. The largest ion observed was  $m/z$  811, and the most abundant ion observed was  $m/z$  420. The ions in the mass spectrum (Figure 5.8) had one signature ion,  $m/z$  387, corresponding to the mass of 3OHKynG. However this ion cannot be 3OHKynG, since the lens protein has been acid hydrolysed, and the glucose molecule hydrolyses under those conditions. MS/MS was conducted on some of the other ions.



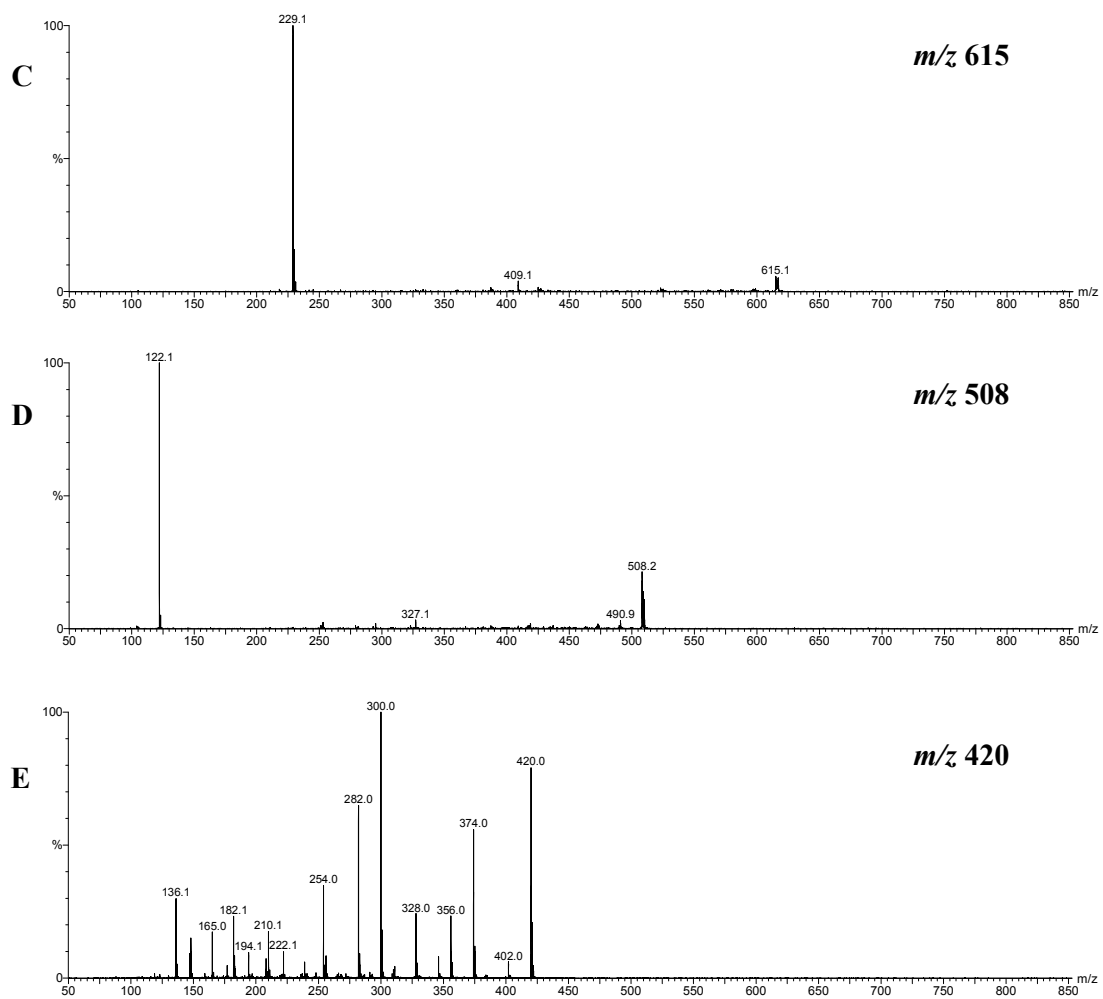
**Figure 5.8** ESI mass spectrum of the sharp peak eluting at 27.8 min in Figure 5.6.

## Chapter 5

Figure 5.9A shows the MS/MS spectrum of ion  $m/z$  806. The fragment ion includes  $m/z$  420. Figure 5.9B shows the MS/MS spectrum of ion  $m/z$  713. The major fragment ions include  $m/z$  668, 622, 429, 409, 387, 327, 267 and 105. Figure 5.9C shows the MS/MS spectrum of ion  $m/z$  615. The major fragment ions include  $m/z$  409 and 229. Figure 5.9D shows the MS/MS spectrum of ion  $m/z$  508. The fragment ions include  $m/z$  327 and 122. Finally, Figure 5.9E shows the MS/MS spectrum of ion  $m/z$  420. Fragment ions include  $m/z$  402, 374, 356, 328, 300, 282, 254, 239, 222, 210, 194, 182, 165, 148 and 136.



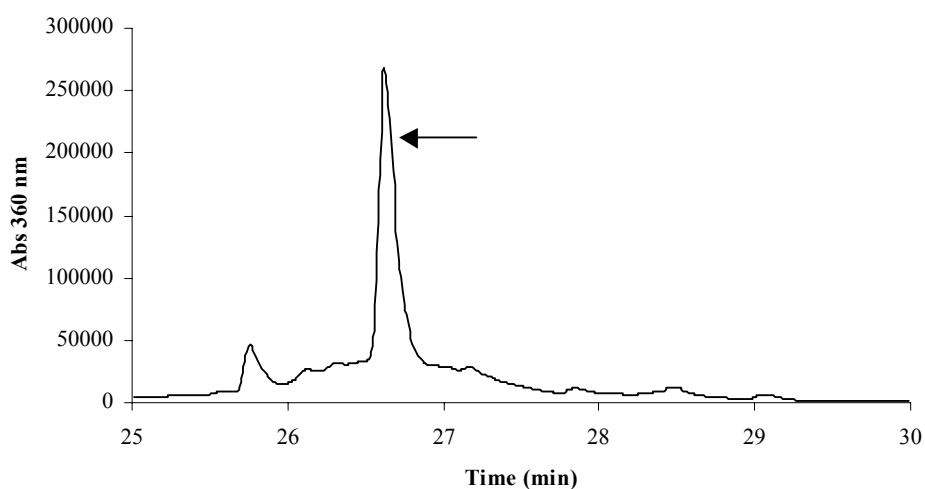




**Figure 5.9** MS/MS spectra. MS/MS of ions that were present in the ESI mass spectrum (Figure 5.8). *A*,  $m/z$  806; *B*,  $m/z$  713; *C*,  $m/z$  615; *D*,  $m/z$  508; *E*,  $m/z$  420.

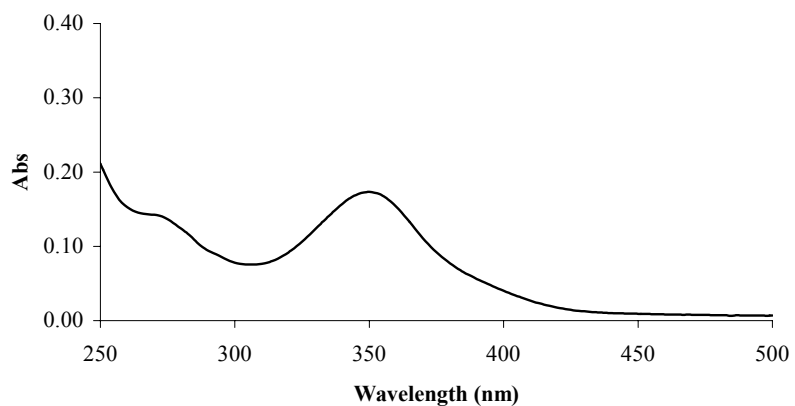
### 5.3.3 Analysis of P3

Acid hydrolysis of human cataract lenses also yielded P3 eluting at 32.2 min (Figure 5.1C). This peak eluted as part of a 'doublet' however the left hand peak of the 'doublet' was not present in the HPLC chromatogram of normal human aged lenses or CLP (Figure 5.1B and Figure 5.1A, respectively) hence, it was of interest for further investigation. P3 was further purified see Section 5.2.5 for details. Figure 5.10 shows the partial HPLC profile of the second stage of HPLC purification, where P3 eluted as a sharp peak at 26.6 min (Figure 5.10). The peak was collected for UV-visible and mass spectral analysis.



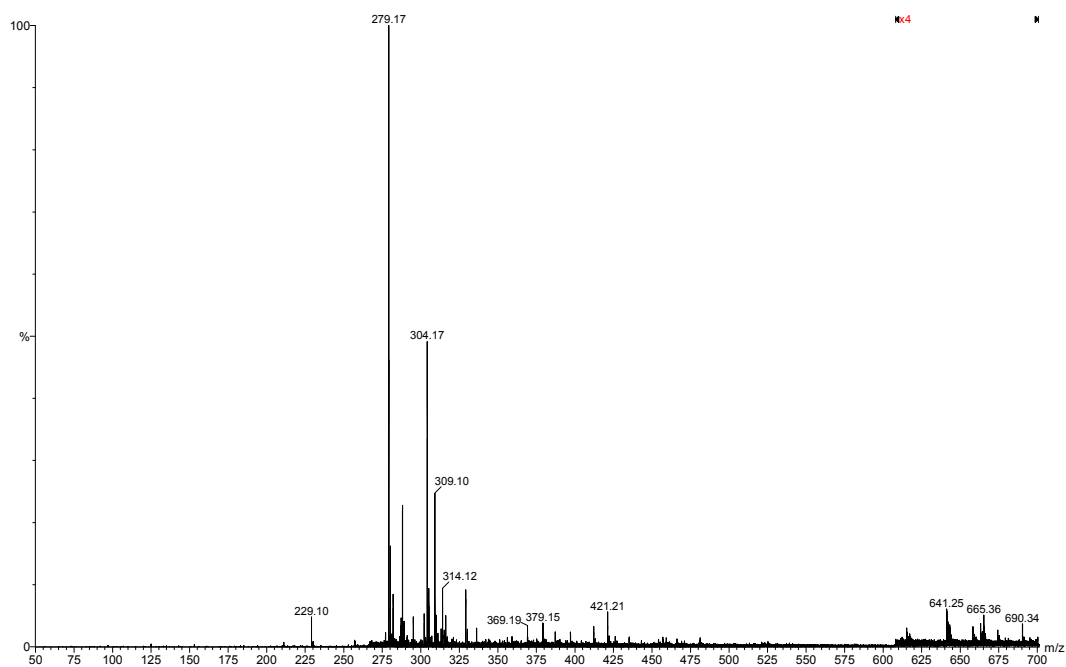
**Figure 5.10** HPLC chromatogram of P3 after a second purification stage. The single peak eluting at 26.6 min was collected for analysis by UV-visible and mass spectrometry.

A UV-visible spectrum of the peak eluting at 26.6 min in Figure 5.10 shows that this product had a broad peak with a maximum absorbance centred at 350 nm (Figure 5.11). The UV-visible spectrum (Figure 5.11) indicates that the product could be a UV filter derivative, however UV filter adducts have a broad peak with a maximum absorbance centred at slightly longer wavelengths (365 nm).



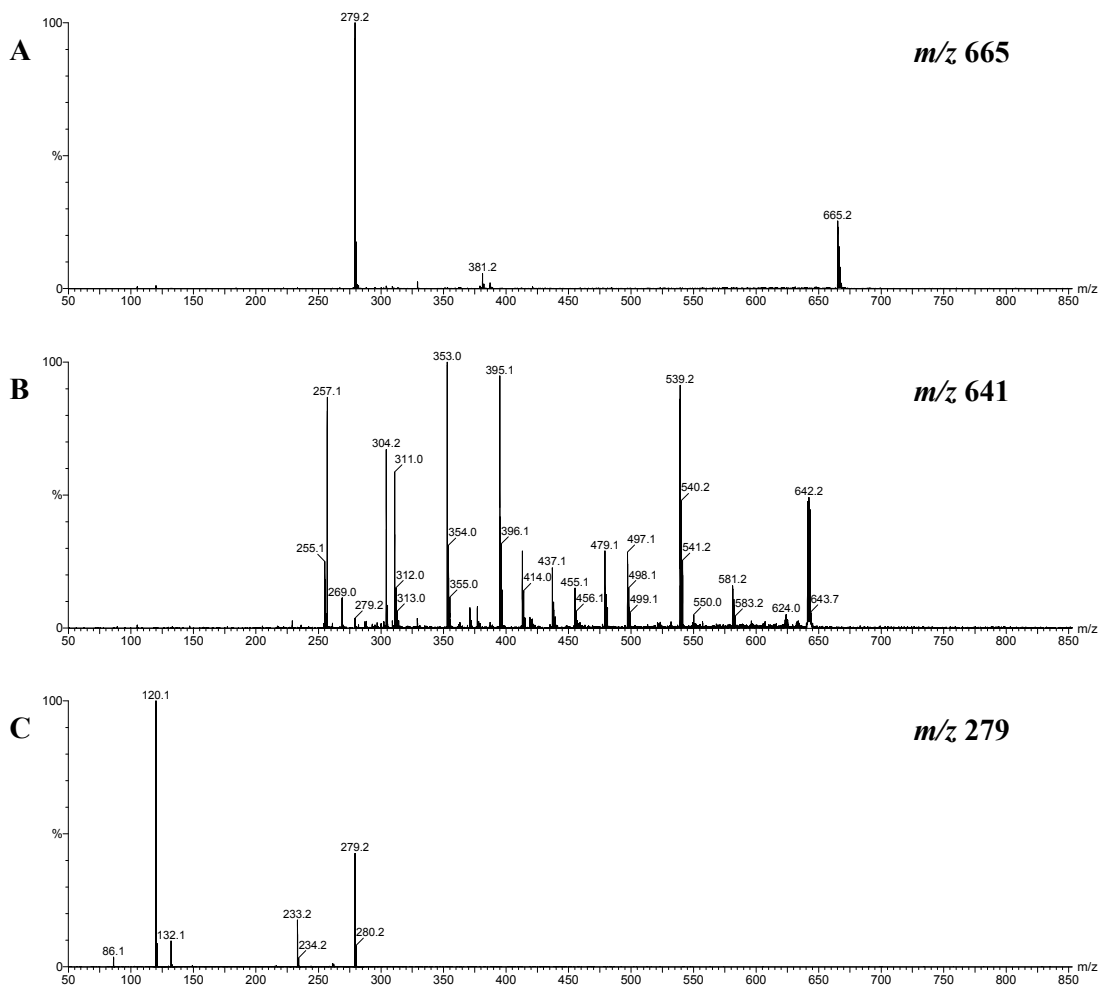
**Figure 5.11** UV-visible spectrum of the peak eluting at 26.6 min in Figure 5.10.

The ESI mass spectrum of the peak eluting at 26.6 min (Figure 5.10) is shown in Figure 5.12. There were no ions greater than  $m/z$  700. The largest ion observed was  $m/z$  690, and the most abundant ion observed was  $m/z$  279. MS/MS was conducted on some of the ions.



**Figure 5.12** ESI mass spectrum of the peak eluting at 26.6 min in Figure 5.10.

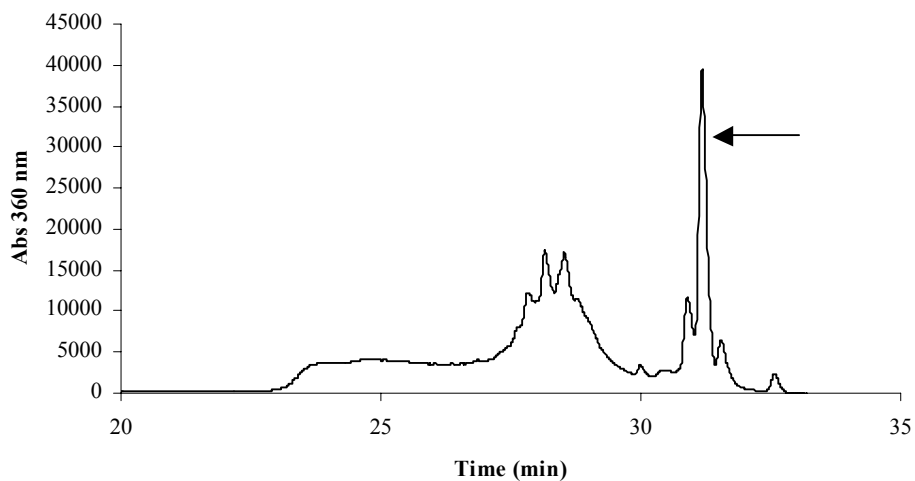
Figure 5.13A shows the MS/MS spectrum of ion  $m/z$  665. The major fragment ions include  $m/z$  381 and 279. Figure 5.13B shows the MS/MS spectrum of ion  $m/z$  641. The major fragment ions include  $m/z$  624, 581, 539, 497, 479, 455, 437, 413, 395, 353, 311, 304 and 257. Figure 5.13C shows the MS/MS spectrum of ion  $m/z$  279. The major fragment ions include  $m/z$  233, 132, 120 and 86.



**Figure 5.13** MS/MS spectra. MS/MS of ions that were present in the ESI mass spectrum (Figure 5.12). *A*,  $m/z$  665; *B*,  $m/z$  641; *C*,  $m/z$  279.

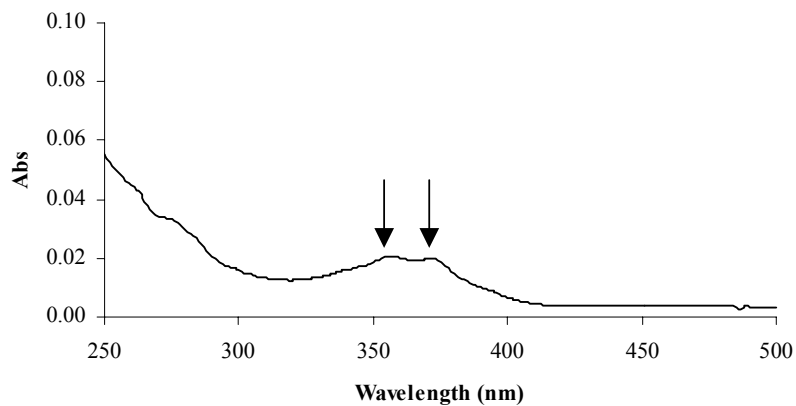
### 5.3.4 Analysis of P4

Acid hydrolysis of human cataract lenses also yielded P4 eluting at 36.0 min (Figure 5.1C). This peak eluted as a small peak in the HPLC chromatogram (Figure 5.1C). P4 was further purified. Figure 5.14 shows the partial HPLC profile of the second phase of HPLC purification. P4 resolved as several minor peaks, but only the major peak eluting at 31.1 min (Figure 5.14) was collected for UV-visible and mass spectral analysis.



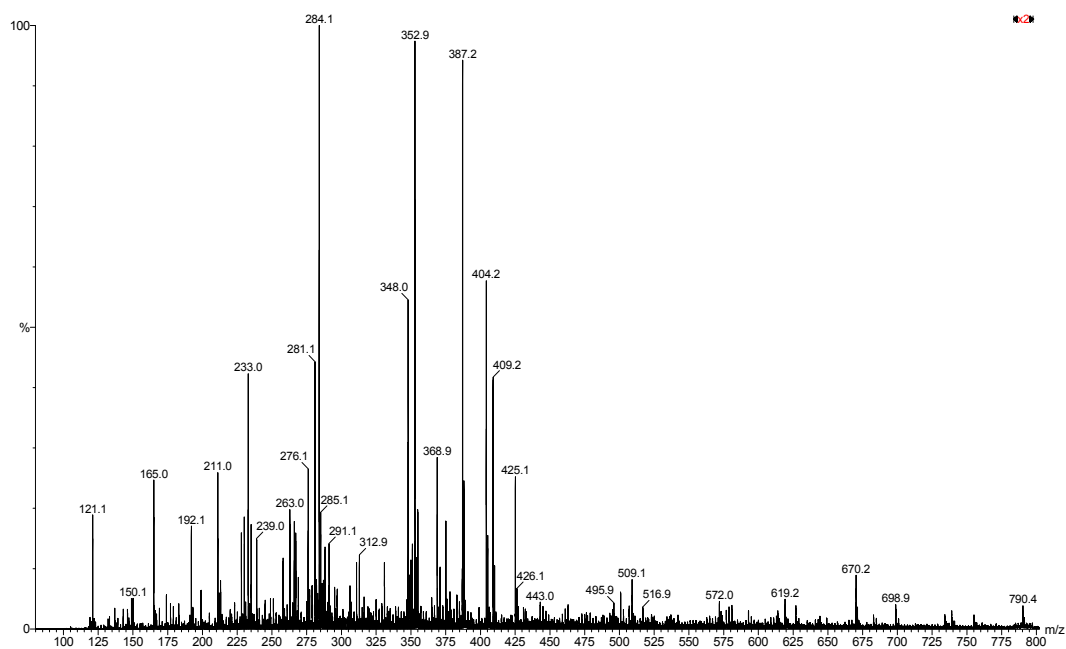
**Figure 5.14** HPLC chromatogram of P4 after a second purification stage. The single peak eluting at 31.1 min was collected for analysis by UV-visible and mass spectrometry.

A UV-visible spectrum of the peak eluting at 31.1 min in Figure 5.14 shows that this product had maximum absorbances centred at 357 and 374 nm (Figure 5.15). The UV-visible spectrum (Figure 5.15) shows that the product could be a UV filter derivative, since UV filter adducts exhibit broad UV absorbances centred at 365 nm.



**Figure 5.15** UV-visible spectrum of the peak eluting at 31.1 min in Figure 5.14.

The ESI mass spectrum of the sharp peak eluting at 31.1 min (Figure 5.14) is shown in Figure 5.16. There were no ions greater than  $m/z$  800. The largest ion observed was  $m/z$  790, and the most abundant ion observed was  $m/z$  284. The ESI mass spectrum exhibits one signature UV filter ion,  $m/z$  192, which corresponds to the mass of Kyn-yellow.<sup>109</sup>



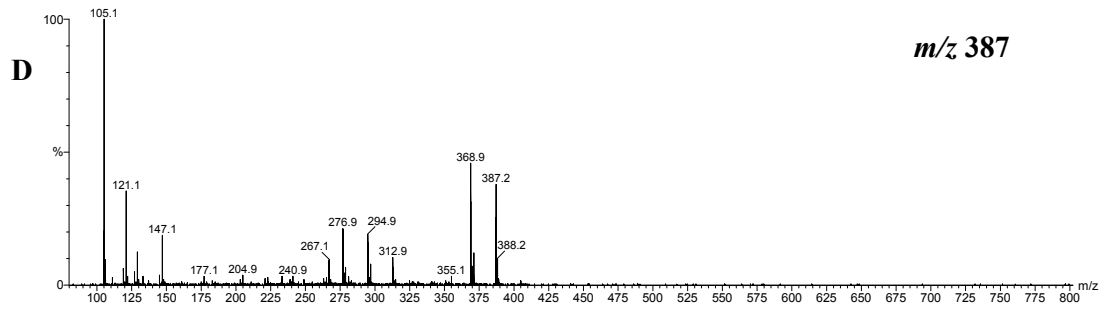
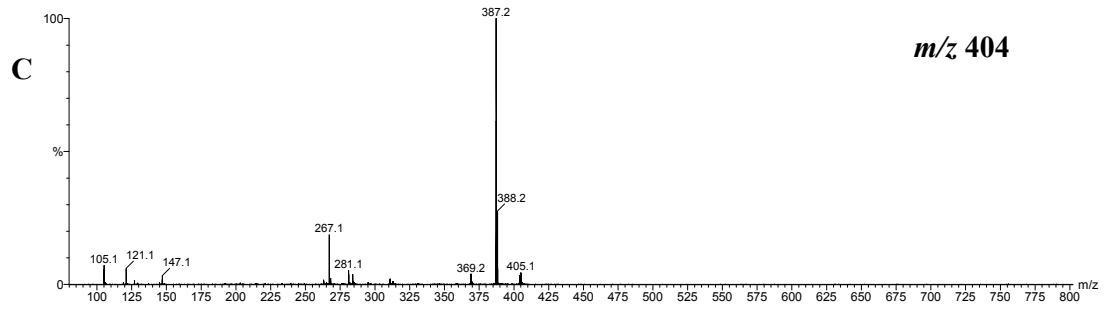
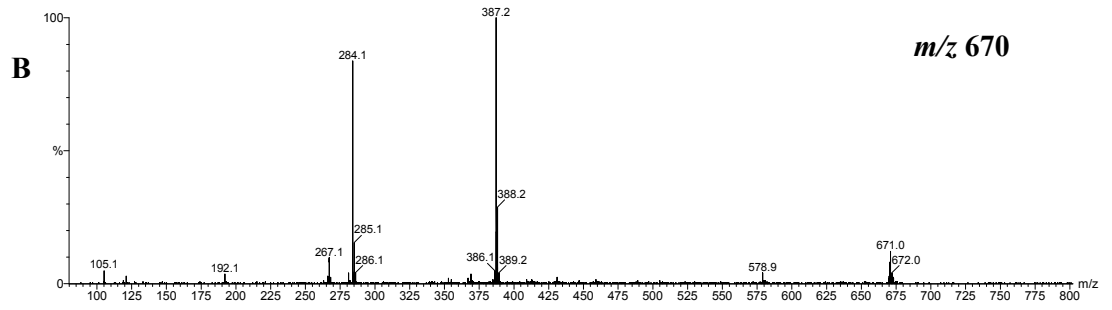
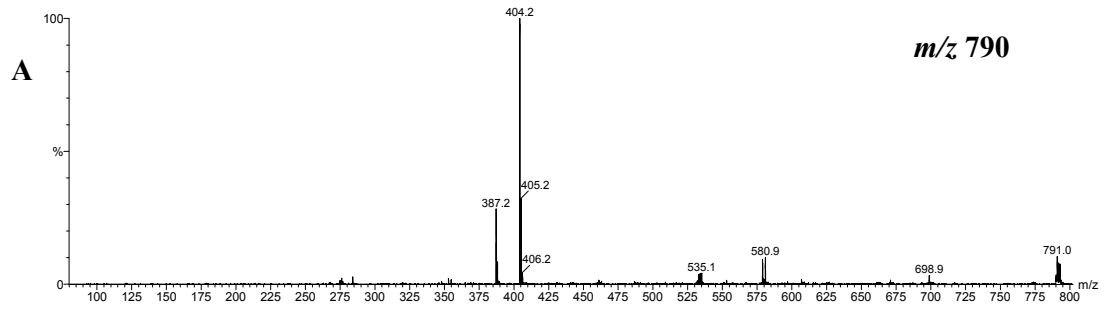
**Figure 5.16** ESI mass spectrum of the peak eluting at 31.1 min in Figure 5.14.

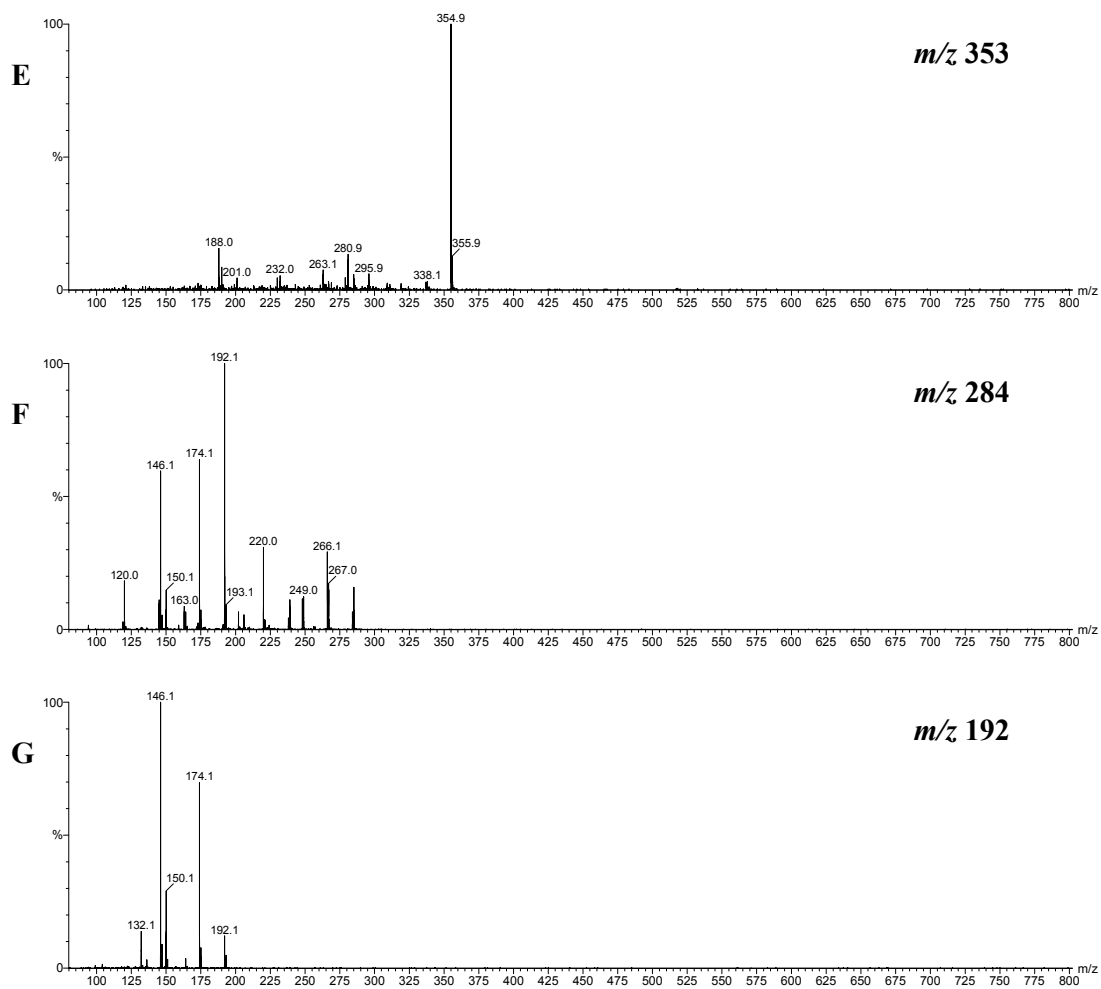


Figure 5.17A shows the MS/MS spectrum of ion  $m/z$  790. MS/MS revealed that the molecule split into two fragments,  $m/z$  404 and 387. Figure 5.17B shows the MS/MS spectrum of ion  $m/z$  670. The major fragment ions include  $m/z$  579, 387, 284, 267, 192 and 105. Figure 5.17C shows the MS/MS spectrum of ion  $m/z$  404. The major fragment ions include  $m/z$  387, 369, 281, 267, 147, 121 and 105. Figure 5.17D shows the MS/MS spectrum of ion  $m/z$  387. The fragment ions include,  $m/z$  369, 313, 295, 277, 267, 147, 121 and 105. Figure 5.17E shows the MS/MS spectrum of ion  $m/z$  353. The fragment ions include,  $m/z$  338, 296, 281, 263, 232, 201 and 188. Figure 5.17F shows the MS/MS spectrum of ion  $m/z$  284. The major fragment ions include  $m/z$  266, 249, 220, 192, 174, 146 and 120. Figure 5.17G shows the MS/MS spectrum of ion  $m/z$  192. The fragment ions include  $m/z$  174, 146 and 132.

The ions  $m/z$  192, 174 and 146 are characteristic fragment ions of Kyn.<sup>103</sup> High resolution mass spectrometric data was obtained for these ions to determine the elemental compositions. Ion  $m/z$  192, 192.0678, calculated for  $C_{10}H_{10}NO_3$ , 192.0661 (mass of Kyn-yellow) and ion  $m/z$  174, 174.0569, calculated for  $C_{10}H_8NO_2$ , 174.0555 (mass of Kyn-yellow minus a water) both correspond to the correct elemental compositions for these fragment compounds of Kyn. Ion  $m/z$  146, 146.0621, calculated for  $C_4H_{10}N_4S$ , did not match that of the expected Kyn fragment. The presence of the ions,  $m/z$  192 and 174 is significant since it shows that P4 could contain a Kyn-derived moiety. As a result of the MS/MS data, it appears that the precursor ion of this Kyn-derived compound is  $m/z$  670, since MS/MS of this ion resulted in two major parts, fragment ions 387 and 284. MS/MS of  $m/z$  284 yielded fragment ions  $m/z$  192 and 174.

Chapter 5





**Figure 5.17** MS/MS spectra. MS/MS of ions that were present in the ESI mass spectrum (Figure 5.16). *A*,  $m/z$  790; *B*,  $m/z$  670; *C*,  $m/z$  404; *D*,  $m/z$  387; *E*,  $m/z$  353; *F*,  $m/z$  284; *G*,  $m/z$  192.

*NMR of P4*

Since the structure of the product P4 could not be identified from the mass spectral data alone, additional human cataract lenses were acid hydrolysed, purified and analysed by nano-NMR spectroscopy. The product (< 1 mg) was dissolved in 50  $\mu$ L of acidified D<sub>2</sub>O, and the solution appeared very coloured (dark yellow). NMR analysis unfortunately showed that there was insufficient sample to complete even the basic NMR experiments needed for structural analysis.

The proton NMR spectrum is shown in Figure 5.18. The spectrum shows that this isolated compound (Figure 5.18) is still impure, since there are numerous broad peaks on the baseline in the spectrum. The HPLC chromatogram (Figure 5.14) also shows that this compound may still be impure following the second stage of HPLC purification, since there are several peaks that elute close together. The proton NMR experiment was undertaken for 16 hours on a 500 MHz NMR spectrometer. The structure of the Kyn amino acid adducts and their proton NMR assignments are known, therefore, an attempt was made to assign some of the peaks (e.g. aromatic protons) in Figure 5.18 on this basis. The ring for Kyn has 4 aromatic hydrogens (Kyn-Lys,  $\delta$ H 7.72 (doublet of doublets (dd)), 7.31 (doublet of doublet of doublets (ddd)), 6.77 (doublet (d)), 6.70 (dd); Kyn-His,  $\delta$ H 7.71 (dd), 7.27 (ddd), 6.72 (d), 6.67 (dd); Kyn-Cys,  $\delta$ H 8.01 (dd), 7.56 (ddd), 7.27 (d), 7.19 (d)).<sup>103</sup> In Figure 5.18, there are 4 doublets at 7.35, 7.29, 7.22 and 6.92 ppm. However, the peak at 6.92 ppm appears to be overlapping with other protons. Integration of the spectrum showed that the doublets at 7.22 and 6.92 ppm corresponded to the same number of protons. The coupling constants for each of the peaks at 7.22 and 6.92 ppm was 9 Hz, indicating that the protons are *ortho* coupled and part of a *para*-disubstituted aromatic ring. The remaining peaks in the proton NMR spectrum were difficult to assign since the structure of this product is unknown.

A gCOSY experiment was undertaken to show the coupling between the hydrogens in the structure. This experiment was undertaken for 16 hours, and after that time only two peaks were exhibited in the aromatic region of the spectrum (Figure 5.19). The two peaks in Figure 5.19B show that the protons at 7.22 and 6.92 ppm couple to each other.

The NMR spectra (Figure 5.18 and Figure 5.19) demonstrate that there was insufficient material for proper structural elucidation of P4.

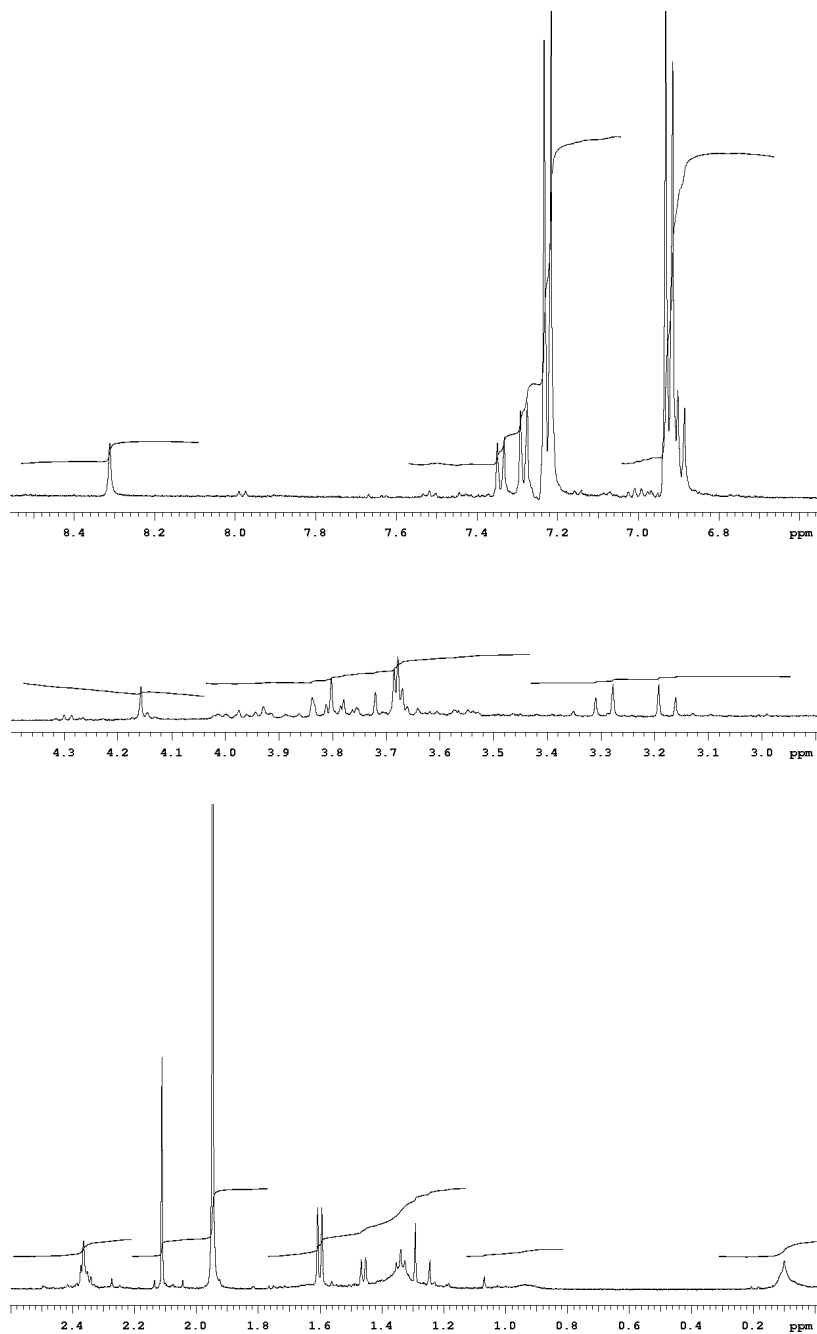


**Figure 5.18** Proton NMR spectrum of the peak eluting at 31.1 min in Figure 5.14.

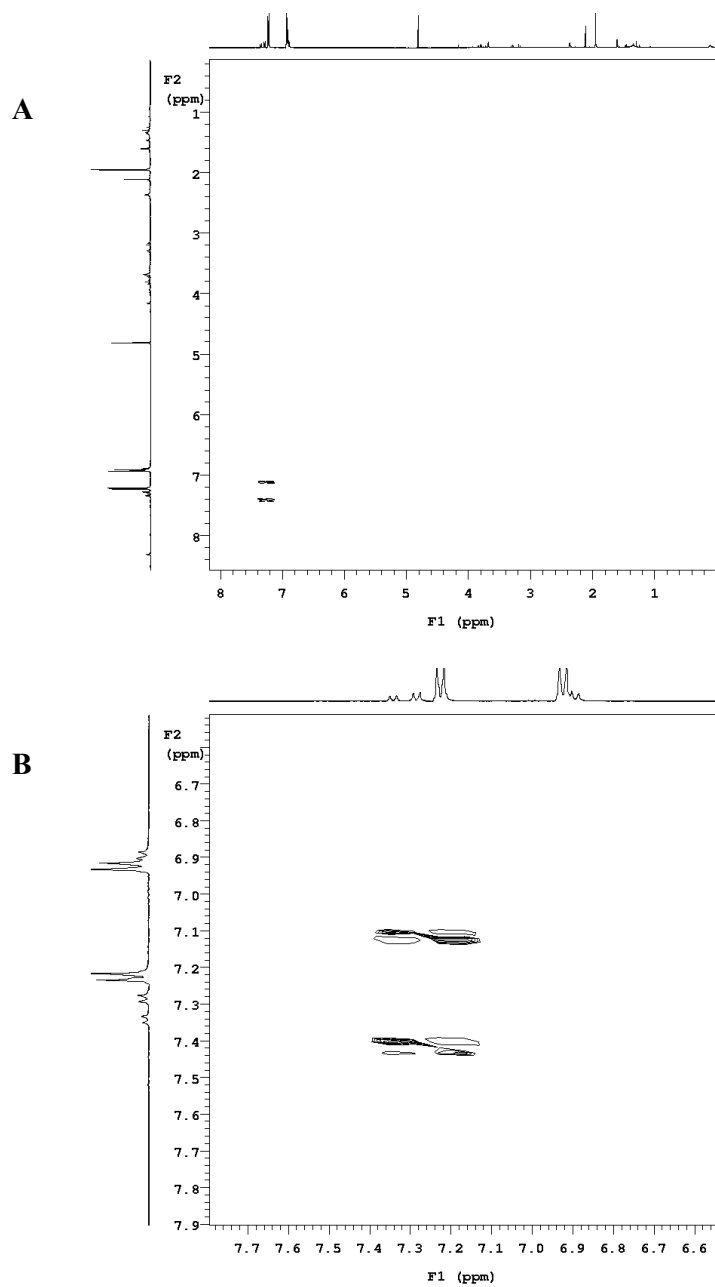


**Figure 5.19** gCOSY spectrum of the peak eluting at 31.1 min in Figure 5.14. *A*, Entire gCOSY spectrum; *B*, Aromatic region of the gCOSY spectrum.

### 5.3.5 Analysis of P5

Acid hydrolysis of human cataract lenses also yielded P5 eluting at 37.5 min (Figure 5.1C). P5 was further purified. Figure 5.20 shows the partial HPLC profile of the second phase of HPLC purification. P5 resolved as many minor peaks, but the major peak eluting at 34.5 min (Figure 5.20) was collected for UV-visible and mass spectral analysis.

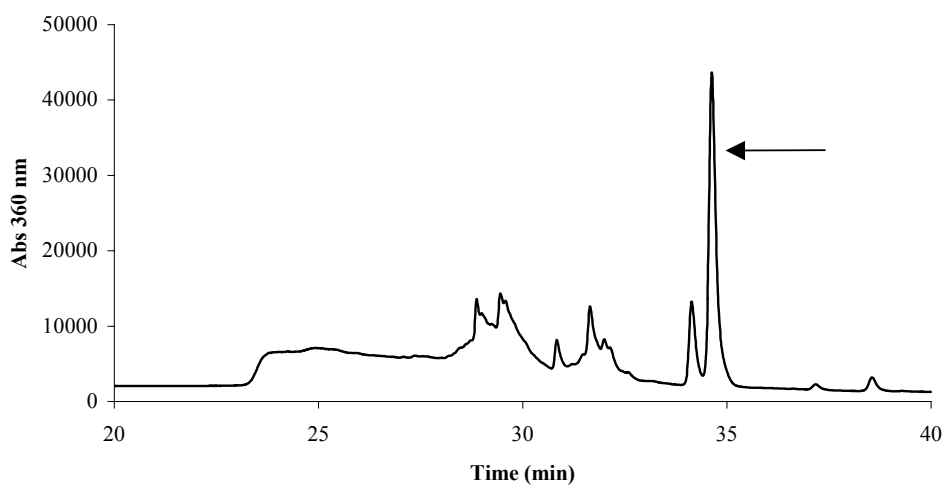


**Figure 5.20** HPLC chromatogram of P5 after a second purification stage. The single peak eluting at 34.5 min was collected for analysis by UV-visible and mass spectrometry.

A UV-visible spectrum of the peak eluting at 34.5 min in Figure 5.20 shows that this product had maximum absorbances centred at 300, 361 and 378 nm (Figure 5.21). The UV-visible spectrum (Figure 5.21) shows that the product may be a UV filter derivative since UV filter adducts exhibit UV absorbances centred at 365 nm.

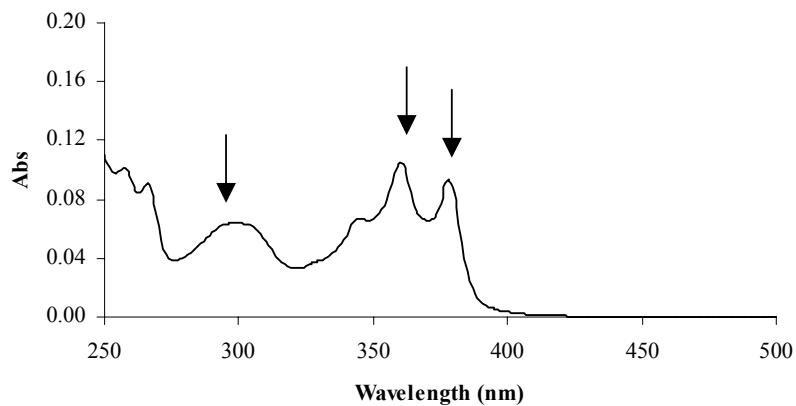


**Figure 5.21** UV-visible spectrum of the peak eluting at 34.5 min in Figure 5.20.



The ESI mass spectrum of the sharp peak eluting at 34.5 min (Figure 5.20) is shown in Figure 5.22. There were no ions greater than  $m/z$  1000. The largest ion observed was  $m/z$  993, and the most abundant ion observed was  $m/z$  607.

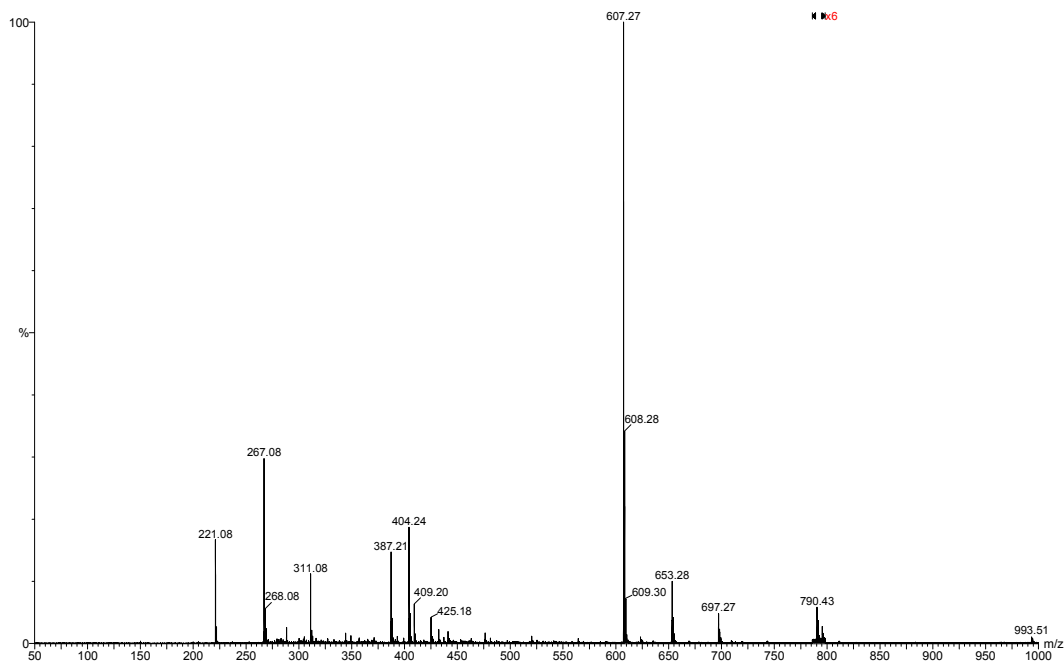


**Figure 5.22** ESI mass spectrum of the peak eluting at 34.5 min in Figure 5.20.

Figure 5.23A shows the MS/MS spectrum of ion  $m/z$  993. The major fragment ions include  $m/z$  607 and 221. Figure 5.23B shows the MS/MS spectrum of ion  $m/z$  790. The major fragment ions include  $m/z$  404, 387 and 221. Figure 5.23C shows the MS/MS spectrum of ion  $m/z$  697. The major fragment ion observed was  $m/z$  311. Figure 5.23D shows the MS/MS spectrum of ion  $m/z$  607. The fragment ions include  $m/z$  387 and 221.

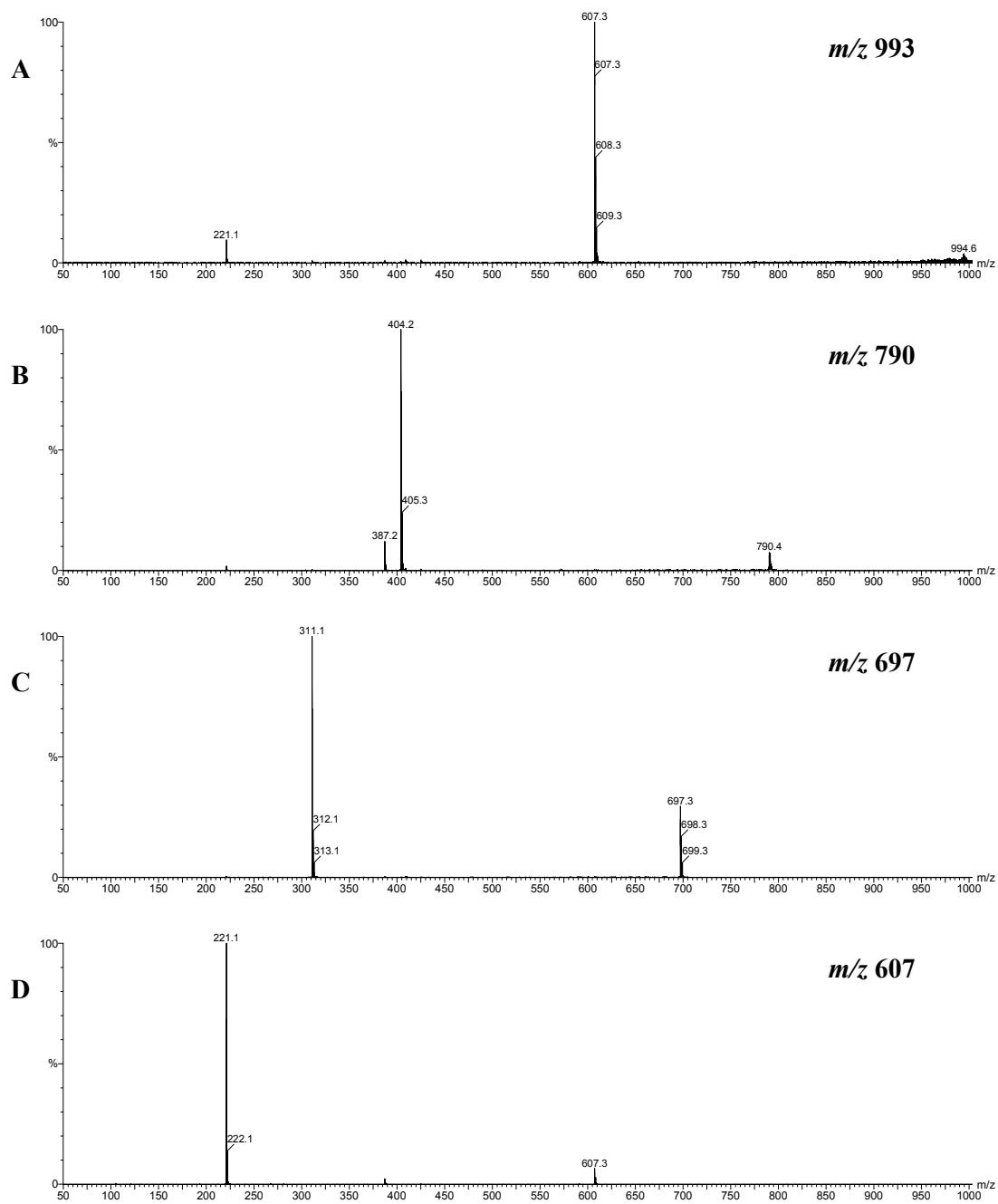


**Figure 5.23** MS/MS spectra. MS/MS of ions that were present in the ESI mass spectrum (Figure 5.22). A,  $m/z$  993; B,  $m/z$  790; C,  $m/z$  697; D,  $m/z$  607.

### 5.3.6 Analysis of P6

P6 was purified by Dr Peter Hains, and he provided the HPLC chromatogram of the second and third stage of HPLC purification, and the mass spectrum of the compound. P6 eluted at 45.0 min on the HPLC chromatogram in Figure 5.1C. P6 was purified twice after the initial HPLC purification, see Sections 5.2.5.3 and 5.2.5.4 for details. The HPLC chromatogram of the second phase of HPLC purification is shown in Figure 5.24A. The HPLC buffers contained heptafluorobutyric acid instead of TFA. The large peak eluting at 42.5 min (Figure 5.24A) was collected and purified further. The HPLC chromatogram of the third phase of HPLC purification is shown in Figure 5.24B. The HPLC buffers contained formic acid at this final stage of HPLC purification. The two large peaks eluting as a doublet at 28 min (Figure 5.24B) were collected, and the mass spectrum of these two peaks are shown in Figure 5.24C. The mass spectrum shows an abundant ion at  $m/z$  367, and the largest ion observed is  $m/z$  734. The mass spectrum did not exhibit any characteristic UV filter ions.

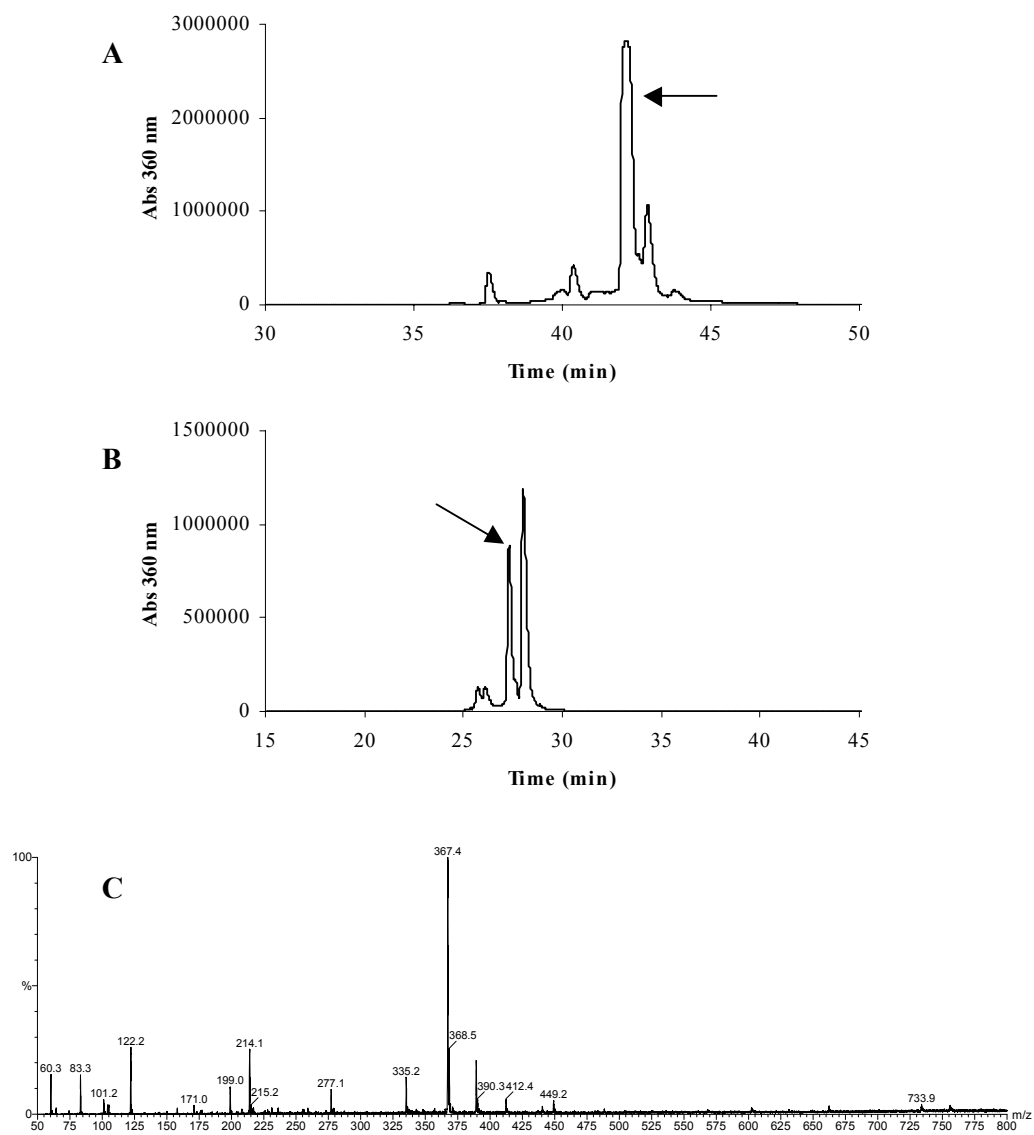


**Figure 5.24** Purification of P6. *A*, HPLC chromatogram of second purification (see Section 5.2.5.3 for details); *B*, HPLC chromatogram of third purification (see Section 5.2.5.4 for details); *C*, ESI mass spectrum of the peaks eluting as a doublet at 28 min in Figure 5.24B.

## 5.4 Discussion

The aim of this study was to see if unusual peaks could be observed in acid digests of cataract lens proteins. If so, this may enable us to draw conclusions as to the species involved in protein modifications in cataract. Another key aim was to obtain structural information on these species, and see, if they may be related to the 3OHKyn or Kyn amino acid adducts. Previous studies, together with the results presented in Chapter 3 of this thesis, show that the three Kyn UV filters, 3OHKynG, 3OHKyn and Kyn, are all attached to the proteins of normal aged human lenses.<sup>101,103</sup> ARN cataract is characterised by oxidation, colouration, insolubilisation and crosslinking of the proteins in the lens.<sup>14,157-160</sup> Cataract lenses differ from normal lenses, which, for example, do not contain oxidised amino acid residues, and normal lenses, whilst yellow, are not as colourised as cataract lenses. It has been proposed that oxidation of protein-bound UV filters may be an important factor in the formation of ARN cataract.

In this study, the HPLC profile of the hydrolysate of human cataract protein was found to differ greatly from the HPLC profiles of acid hydrolysed CLP and acid hydrolysed normal human aged lens protein (Figure 5.1). It was of particular interest to examine the properties of the novel peaks in the HPLC profile of acid hydrolysed cataract lenses that eluted at 360 nm wavelength. This wavelength was chosen since Kyn UV filters exhibit maximum UV-visible absorbances centred at 365 nm.<sup>102</sup> Breakdown products of UV filters, which absorb at other wavelengths would not be not detected. HCl is known to cause Trp to breakdown to Kyn.<sup>209</sup> This is an important consideration, however controls were incorporated into this study, *i.e.* the cataract hydrolysates were compared to the hydrolysates of CLP and normal aged human lens protein. In addition antioxidants, phenol and thioglycolic acid, were added to the acid during hydrolysis. However, antioxidants do not entirely prevent Trp breakdown.

Hydrolysis of cataract lens nuclear proteins resulted in the elution of six significant peaks (P1, P2, P3, P4, P5, and P6) in the HPLC chromatogram (Figure 5.1C), that were not present in the hydrolysate of normal aged lens proteins (Figure 5.1B). These were observed consistently in different batches of cataract lenses. Each peak was collected, and rerun on HPLC for purity. UV-visible spectroscopy was used to detect if peaks

resembled UV filters. Mass spectrometry was employed to identify UV filter ions, and NMR spectroscopy was employed for structural elucidation of P4.

The UV-visible spectra for each of the peaks, P1, P2, P3, P4 and P5, showed that the product in each of the peaks was possibly a UV filter derivative, since absorbance was broad and centred at 360-370 nm in each of the UV-visible spectra. The UV-visible spectrum of P1 (Figure 5.3) and P2 (Figure 5.7) were fairly similar *i.e.* broad peaks with maximum absorbances centred at 360 nm. These two UV-visible spectra are comparable to the UV-visible spectra for each of the 3OHKyn amino acid adducts at acidic and neutral pH (Chapter 2 of this thesis). The UV-visible spectra of P1 and P2 are also comparable to the UV spectra of the Kyn amino acid adducts.<sup>103</sup> Therefore, P1 and P2 may be derived from UV filters. The UV-visible spectrum of P3 varied slightly to that of P1 and P2. The maximum absorbance of P3 was centred at 350 nm (Figure 5.11), although the absorbance is lower in wavelength than that expected for UV filters (360-370 nm), the shape of the curve in the UV-visible spectrum suggests that P3 could also be a UV filter derivative. The UV-visible spectra of P4 (Figure 5.15) and P5 (Figure 5.21) were distinctly different to those of P1, P2 and P3. Maximal absorbance was still centred in the 360-370 nm range, however, two maximal absorbances were observed in that wavelength region. Therefore, the chromophore of P4 and P5 could be very similar to each other, but different to the chromophores of P1, P2 and P3. P4 and P5 may still be UV filter derivatives since such ‘double peak’ absorbances are characteristic of phenoxazone compounds, for example, xanthommatin<sup>184</sup> that are formed by oxidation of 3OHKyn or 3-hydroxyanthranilic acid. No UV-visible data was available for P6. In summary, the UV-visible spectra showed that the novel peaks isolated from the cataract lenses could all be UV filter derived compounds.

Mass spectrometry was employed to identify ‘signature’ UV filter ions in each of the novel peaks. Since the protein was acid hydrolysed, ions related to Kyn (Kyn-His,  $m/z$  347; Kyn-Lys,  $m/z$  338; Kyn-Cys,  $m/z$  313<sup>103</sup>) or 3OHKyn adduct ions (3OHKyn-His,  $m/z$  363; 3OHKyn-Lys,  $m/z$  354; 3OHKyn-Cys,  $m/z$  329) were expected, but not fragment ions from 3OHKynG, since acid hydrolysis cleaves the glucose from 3OHKynG. Table 5.1 lists the Kyn and 3OHKyn amino acid adduct ‘signature’ ions

and, Table 5.2 is a summary of all of the ions and fragment ions that were identified in each of P1, P2, P3, P4, P5 and P6. Ions in Table 5.1 were generally not observed in Table 5.2 *i.e.* the characteristic ions of the UV filters adducts were not present in any of the ESI mass spectra of the novel compounds, except for the ESI mass spectrum of P4 (Figure 5.16), which had a low abundance  $m/z$  313 ion (theoretical mass of Kyn-Cys<sup>103</sup>).

The ESI and MS/MS mass spectra of P1, P2 and P3 did not show any familiar ‘signature’ ions, and structural elucidation was not possible from mass spectral data alone. The ESI mass spectrum of P6 again did not show any UV filter ‘signature’ ions.

Kyn ‘signature’ ions were identified in the ESI and MS/MS spectra of P4. Apart from the  $m/z$  313 ion in the ESI spectrum,  $m/z$  192 was also present (Kyn fragment ion). MS/MS of the higher molecular weight ions in the ESI spectrum showed that, MS/MS of  $m/z$  670 yielded fragment ions  $m/z$  579, 387, 284, 267, 192 and 105. MS/MS of  $m/z$  192 yielded  $m/z$  174 and 146 which are both fragment ions of Kyn.<sup>103</sup> MS/MS of  $m/z$  387, resulted in fragment ions,  $m/z$  369, 313, 295, 277, 267, 147, 121 and 105. If ion  $m/z$  313 were that of Kyn-Cys (theoretical molecular ion), then MS/MS of  $m/z$  387 should yield fragment ions of Kyn-Cys which include  $m/z$  295, 224, 202, 192, 174, 146 and 122.<sup>103</sup> Since these fragment ions were not present, Kyn-Cys is not a component of P4, but P4 very likely consists of a Kyn derivative, since high resolution mass spectrometric data of ions,  $m/z$  192 and 174 resulted in the expected elemental compositions for these two characteristic Kyn fragment ions. In summary, the source for the unknown Kyn derivative in P4 appears to be  $m/z$  670. NMR analysis of P4 showed that there was insufficient sample for structural elucidation but showed that P4 was an aromatic molecule.

The ESI mass spectrum of P5 showed that there was an ion  $m/z$  790, which was also present in the ESI mass spectrum of P4. MS/MS of  $m/z$  790 (in P5) resulted in fragment ions 404 and 387 (Figure 5.23B), and MS/MS of  $m/z$  790 (in P4) also resulted in the same two fragment ions (Figure 5.17A), and both ions appeared in the similar ratio as that observed in P5 *i.e.*  $m/z$  404 was the most abundant (100%), and  $m/z$  387 was at 15-

25% the abundance of the  $m/z$  404 ion. Therefore, it is very likely that a component of P4 and P5 are closely related in structure.

Because it is likely that oxidation of UV filters has taken place during ARN cataract formation, it may not be surprising that ions characteristic of unoxidised UV filters were absent. The ions of the expected 3OHKyn crosslink compounds in Chapter 4, Table 4.4, were also not observed in any of the ESI or MS/MS spectra of P1-P6. In addition, the HPLC profile of hydrolysed cataract lens protein (Figure 5.1C) was not comparable to the HPLC profiles of oxidised 3OHKyn-modified protein (Figure 4.24B and Figure 4.32B), *i.e.* there was no similarity in the pattern of the peaks that eluted in the hydrolysate of cataract protein and 3OHKyn-modified protein.

In this study, the aim was to hydrolyse cataract lens proteins and identify novel compounds. With age, the concentration of the major lens antioxidant, GSH, decreases significantly, especially in the nucleus of the lens.<sup>19,55</sup> The nucleus of a cataract lens is an oxidising environment, and maintenance of adequate GSH levels in the nucleus of the lens is crucial<sup>91,226,227</sup> for minimising polypeptide modifications. Although the isolated compounds could not be structurally characterised, the approach undertaken in this study was shown to be feasible, since in the past, acid hydrolysis of normal aged lens protein has revealed UV filter modifications.<sup>103</sup>

There have been a number of novel modifications reported in the literature. The majority of the studies used acid hydrolysis to isolate the novel compounds from the hydrolysates. Table 5.3 lists the modifications that have been identified in cataract lenses, and the quantitations are also listed (see Figures 1.4 and 1.6 for the structures of the modifications). The absorbance of the UV detector used in the HPLC purification has also been listed. Of all the modifications listed, two studies used enzymatic digestion. Cheng, *et al.* identified K2P,<sup>107</sup> and Ahmed, *et al.* identified MG-H1 and MG-H2<sup>130</sup> using enzymatic digestion of cataractous lens proteins. Although enzymatic digestion is a 'gentler' method, a disadvantage of enzymatic digestion is insufficient digestion of the proteins.



A future aim is to identify oxidised UV filter compounds that survive acid hydrolysis of modified protein, and to compare it with authentic cataract lens digests.

**Table 5.2** Summary of the ions and fragment ions identified in the peaks, P1, P2, P3, P4, P5 and P6, which were isolated and purified from hydrolysed human cataract lens proteins.

<b>Peak</b>	<b>Ions</b>	<b>Fragment Ions</b>
<b>P1</b>	- $m/z$ 658	- $m/z$ 641, 454, 374, 346, 270, 242, 233
	- $m/z$ 505	- $m/z$ 487, 469, 418, 382, 326, 308, 254, 236, 206, 162
	- $m/z$ 419	- $m/z$ 254, 166
	- $m/z$ 331	- $m/z$ 166, 120
	- $m/z$ 270	- $m/z$ 252, 234, 224, 206, 178, 160, 137, 106, 88
	- $m/z$ 166	- $m/z$ 149, 131, 120, 107, 103
<b>P2</b>	- $m/z$ 806	- $m/z$ 420
	- $m/z$ 713	- $m/z$ 668, 622, 429, 409, 387, 327, 267, 105
	- $m/z$ 615	- $m/z$ 409, 229
	- $m/z$ 508	- $m/z$ 327, 122
	- $m/z$ 420	- $m/z$ 402, 374, 356, 328, 300, 282, 254, 239, 222, 210, 194, 182, 165, 148, 136
<b>P3</b>	- $m/z$ 665	- $m/z$ 381, 279
	- $m/z$ 641	- $m/z$ 624, 581, 539, 497, 479, 455, 437, 413, 395, 353, 311, 304, 257
	- $m/z$ 279	- $m/z$ 233, 132, 120, 86
<b>P4</b>	- $m/z$ 790	- $m/z$ 404, 387
	- $m/z$ 670	- $m/z$ 579, 387, 284, 267, 192, 105
	- $m/z$ 404	- $m/z$ 387, 369, 281, 267, 147, 121, 105
	- $m/z$ 387	- $m/z$ 369, 313, 295, 277, 267, 147, 121, 105
	- $m/z$ 353	- $m/z$ 338, 296, 281, 263, 232, 201, 188
	- $m/z$ 284	- $m/z$ 266, 249, 220, 192, 174, 146, 120
	- $m/z$ 192	- $m/z$ 174, 146, 132
<b>P5</b>	- $m/z$ 993	- $m/z$ 607, 221
	- $m/z$ 790	- $m/z$ 404, 387, 221
	- $m/z$ 697	- $m/z$ 311
	- $m/z$ 607	- $m/z$ 387, 221
<b>P6</b>	- $m/z$ 734	
	- $m/z$ 449	
	- $m/z$ 389	
	- $m/z$ 367	
	- $m/z$ 335	
	- $m/z$ 277	
	- $m/z$ 214	
	- $m/z$ 122	

**Table 5.3** List of modifications in human cataract lens proteins.<sup>104-107,130,212</sup>

See Figures 1.4 and 1.6 for the structures of the modifications